HHS Public Access

Author manuscript

Mol Cell. Author manuscript; available in PMC 2018 January 19.

Published in final edited form as:

Mol Cell. 2017 January 19; 65(2): 207–219. doi:10.1016/j.molcel.2016.12.008.

Programmed ribosomal frameshifting generates a copper transporter and a copper chaperone from the same gene

Sezen Meydan[1], **Dorota Klepacki**[1], **Subbulakshmi Karthikeyan**[1], **Tõnu Margus**[1], **Paul Thomas**[2], **John E. Jones**[3], **Yousuf Khan**[3], **Joseph Briggs**[3], **Jonathan D. Dinman**[3], **Nora Vázquez-Laslop**[1,*], and **Alexander S. Mankin**[1,*]

[1]Center for Biomolecular Sciences – m/c 870, University of Illinois at Chicago, 900 S. Ashland Ave., Chicago, IL 60607, USA

[2]Proteomics Center of Excellence-Northwestern University, 633 Clark S., Chicago, IL 60208, USA

[3]Department of Cell Biology and Molecular Genetics, University of Maryland, College Park, MD 20742, USA

Summary

Metal efflux pumps maintain ion homeostasis in the cell. The functions of the transporters are often supported by chaperone proteins, which scavenge the metal ions from the cytoplasm. Although the copper ion transporter CopA has been known in *Escherichia coli*, no gene for its chaperone had been identified. We show that the CopA chaperone is expressed in *E. coli* from the same gene that encodes the transporter. Some ribosomes translating *copA* undergo programmed frameshifting, terminate translation in the -1 frame, and generate the 70 amino acid-long polypeptide CopA(Z), which helps cells survive toxic copper concentrations. The high efficiency of frameshifting is achieved by the combined stimulatory action of a 'slippery' sequence, an mRNA pseudoknot, and the CopA nascent chain. Similar mRNA elements are not only found in the *copA* genes of other bacteria but are also present in *ATP7B*, the human homolog of *copA*, and direct ribosomal frameshifting in vivo.

Graphical abstract

*Corresponding authors: Lead Contact: Alexander Mankin, Center for Biomolecular Sciences - m/c 870, University of Illinois, 900 S. Ashland Ave., Rm. 3052, Chicago, IL 60607, Phone: 312-413-1406, shura@uic.edu.

Supplemental Information: Supplemental information includes four figures and one table.

Author Contributions: S.M., N. V.-L. and A.S.M. conceived the project, designed the experiments, analyzed the data, wrote the paper; J.D.D., J.E.J. and Y.K. designed some experiments and analyzed the data; S.M., D.K., S.K., T. M., P.T., J.E.J., Y.K., J.B. performed the experiments.

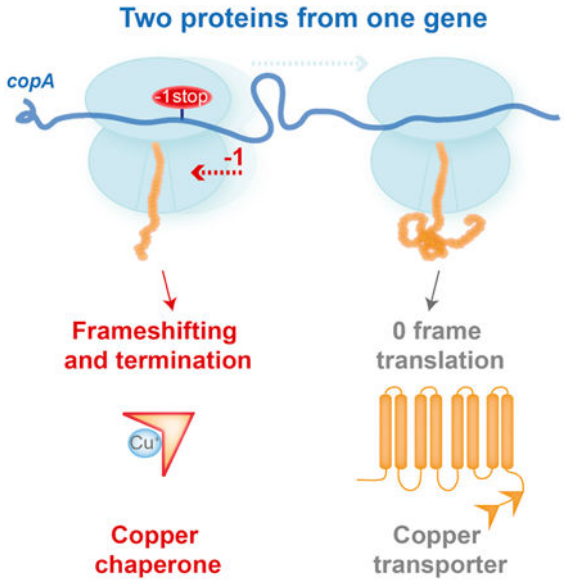

Introduction

Copper homeostasis is critical for organisms from all domains of life. Due to the ability of copper ions to switch between two oxidation states, Cu(I) and Cu(II), copper serves as an essential cofactor for enzymes that participate in key processes including electron transport and the oxidative stress response (Arredondo and Nunez, 2005). In excess however, copper ions are extremely toxic for the cell likely because of their role in generating reactive oxygen species (Rensing and Grass, 2003). Disruption of copper homeostasis has been linked to human maladies e.g., Menkes, Wilson, and Parkinson diseases as well as cystic fibrosis (Bull et al., 1993; Percival et al., 1999; Torsdottir et al., 1999; Vulpe et al., 1993). Sophisticated systems have evolved to maintain copper homeostasis in bacterial and eukaryotic cells (Fan and Rosen, 2002; Outten and O'Halloran, 2001), in which the central role belongs to copper-translocating ATPases responsible for export of excess copper ions from the cell (Fan and Rosen, 2002; Migocka, 2015).

The operation of copper transporters in bacteria often relies on the assistance of metal chaperones (e.g., CopZ in *Bacillus subtilis* and *Enterococcus hirae*). These small soluble proteins facilitate trafficking of copper ions to the transporters and their regulators (Banci et al., 2001; Cobine et al., 1999; Palumaa, 2013). Curiously, while the Cu(I) efflux transporter CopA operates in *Escherichia coli*, a gene for the CopZ-like diffusible chaperone was not identified in its genome (Fan et al., 2001; Rensing et al., 2000). A recent study demonstrated that the copper hypersensitivity caused by the artificial truncation of the N-terminal metal binding domain 1 (MBD1) of the *E. coli* CopA transporter could be compensated *in trans* by expression of the *B. subtilis* CopZ chaperone (Drees et al., 2015). Intriguingly, the same beneficial effect was achieved by ectopic expression of the *E. coli* CopA MBD1 itself, indicating that the N-terminal segment of CopA could potentially provide the copper chaperone function in *E. coli*. However, in contrast to the diffusible metal chaperones found in many organisms (Jordan et al., 2001; Palumaa, 2013), the putative copper chaperone of *E.*

coli, being a part of the CopA protein, has to operate as an integral part of the membrane transporter. Such an arrangement should inevitably restrict the ability of the chaperone to scavenge copper ions from cytosolic locations and deliver them to the membrane-embedded efflux pump.

Several serendipitous observations hinted that expression of the *E. coli copA* gene might deviate from the conventional pathway. Gel analysis of small proteins expressed in *E. coli* revealed the presence of a short polypeptide with an estimated molecular weight (MW) of ca. 6.5 kDa, whose tryptic peptides matched those of the CopA MBD1 (Wasinger and Humphery-Smith, 1998). Although such a protein could be hypothetically generated via proteolytic degradation of the full-size transporter, no evidence for specific cleavage of CopA by cellular proteases has been reported. Even more puzzling, recent ribosome profiling examination of protein synthesis in the *E. coli* strain MG1655 indicated that the number of translating ribosomes abruptly drops in the vicinity of the 70th codon of the *copA* gene (Li et al., 2014). A similar unexplained decrease in ribosome density within *copA* could also be seen in other ribosome profiling datasets collected from various *E. coli* strains and under different growth conditions (Balakrishnan et al., 2014; Elgamal et al., 2014; Guo et al., 2014; Kannan et al., 2014; Li et al., 2014; Mohammad et al., 2016; Oh et al., 2011). This unique pattern of distribution of ribosome progression along the gene suggested that expression of *copA* might be a subject of idiosyncratic regulation.

One of the mechanisms exploited by cells for expanding the spectrum of proteins expressed from a limited number of genomic ORFs is translational recoding (Baranov et al., 2002). This term refers to a variety of scenarios in which interpretation of the genetic information deviates from the straightforward single-frame codon-by-codon translation of mRNA by the ribosomes. Among other options, recoding may involve programmed ribosomal frameshifting (PRF), a forward or backwards slippage of the ribosome to an alternative reading frame within the ORF. PRF conceptually resembles spontaneous frameshift errors, although its frequency is usually significantly higher and could be subjected to specific regulation (Farabaugh and Bjork, 1999; Kurland, 1992). In order to achieve high efficiency of recoding, particular structural features are embedded in mRNA, including PRF-prone ‘slippery sequences’, upstream or downstream stimulatory RNA secondary structures or the presence of internal Shine-Dalgarno-like sequences (Caliskan et al., 2015; Farabaugh, 1996). Two core *E. coli* genes are known to be regulated by PRF. Expression of release factor 2 (RF2) from the *prfB* gene, is controlled by +1 PRF. The PRF frequency depends on the efficiency of translation termination at the premature in-frame stop codon, which in turn requires RF2 activity. Only the full-size release factor, generated as the result of PRF, carries physiologically meaningful cellular function, whereas the truncated, prematurely terminated peptide seems to play no functional role (Craigen and Caskey, 1986). In contrast to *prfB*, the -1 PRF in the *dnaX* gene generates two functional polypeptides corresponding to individual subunits of the same enzyme, DNA polymerase III (Blinkowa and Walker, 1990; Flower and McHenry, 1990; Tsuchihashi and Kornberg, 1990). More recently, it has been shown that -1 PRF in the gene *csoS2* of CO_2-fixating bacteria leads to production of two isoforms of the CsoS2 protein involved in the biogenesis of α-carboxisome. However, the functionality of one of the isoforms still remains unconfirmed (Chaijarasphong et al, 2016).

Here, we show that the *copA* gene in *E. coli* encodes two proteins, likely with related but distinct functions. Translation of the entire gene generates a membrane copper transporter CopA, while -1 PRF leading to premature termination results in synthesis of the 70 amino acid-long copper chaperone CopA(Z). A highly efficient -1 PRF, stimulated by a slippery sequence and specific elements encoded within the mRNA and nascent polypeptide, controls expression of the two polypeptides from a single ORF. The same slippery sequence and a similar downstream mRNA structure are present in the human *ATP7B* gene, which codes for the copper transporter homolog of bacterial CopA, and whose functional defects are implicated in Wilson disease (Bull et al., 1993; Gupta and Lutsenko, 2012). The utilization of PRF by the copper transporter genes illuminates the role of recoding in maintaining the homeostasis of an essential metal in the cell.

Results

In vivo expression of the *copA* gene results in the formation of the 70 amino acid-long CopA(Z)

Ribosome profiling revealed an abrupt decrease of ribosome density in the vicinity of the 70th codon of the *E. coli copA* gene (Balakrishnan et al., 2014; Elgamal et al., 2014; Guo et al., 2014; Kannan et al., 2014; Li et al., 2014; Mohammad et al., 2016; Oh et al., 2011) (Figure 1A). We hypothesized that this unique pattern of *copA* translation could reflect the specific expression of an approximately 70 amino acid residues-long truncated CopA protein via an as yet undefined mechanism. This putative polypeptide would encompass the entire MBD1 of the CopA transporter (Figure 1A) and thus would closely correspond to the N-terminal segment of CopA proposed to serve as a transporter-linked copper chaperone in *E. coli* (Drees et al., 2015). In order to explore whether the N-terminal segment of CopA is indeed synthesized in the cell as an individual polypeptide, we used the *copA*-containing ASKA library plasmid (Kitagawa et al., 2005) to express the N-terminally His_6-tagged CopA (we will refer to this plasmid as pCopA). Introduction of pCopA in the Δ*copA E. coli* strain BW25113 (Baba et al., 2006) led to the appearance of not only the full-size CopA transporter, but also of a polypeptide which migrated in a SDS gel as an approximately 10-12 kDa protein (Figures 1B and 2B). The size of this shorter product, as estimated from its electrophoretic mobility closely matched the predicted MW for the His_6-tagged MBD1 of CopA (~9 kDa). To determine the precise size of the expressed truncated CopA polypeptide, which we named CopA(Z), we purified it using a Ni^{2+} affinity column (Figure 1B) and determined its exact MW by mass spectrometry (Figure 1C). The experimentally determined MW of the expressed His_6-tagged CopA(Z) was 9,323 Da. This value was in a reasonable agreement with the profiling results, where the ribosomal density dropped immediately after the 70th codon; the predicted MW of the polypeptide encoded by the first 70 codons of the *copA* gene would be 9,337 Da. Thus, the results of the mass-spec analysis suggested that a diffusible 70 amino acid-long CopA(Z) protein encompassing MBD1 is expressed from the *copA* gene alongside with the full-size 834-amino acid long CopA, a transmembrane metal transporter. Such a scenario would resolve the mystery of the missing copper chaperone in *E. coli*. However, the mechanism of generation of CopA(Z), as well as the origin of the difference of 14 Da between its predicted and experimentally-determined MWs (Figure 1C) remained puzzling.

PRF resulting in premature termination of translation is responsible for the production of CopA(Z)

We explored the reason for the discrepancy between the predicted and experimentally determined MW of CopA(Z) hoping that it held the clue to the mechanism of its generation. The molecular mass difference between the estimated and experimental CopA(Z) molecular mass could be accounted for by the replacement of the CopA(Z) C-terminal alanine, encoded in the *copA* 70th codon, with glycine (Figure 1C). Such a change could be brought about by a single nucleotide substitution in the 70th codon, converting it from GCT to GGT (Gly). However, neither the chromosomal gene of the parental BW25113 strain, nor the gene present in the pCopA plasmid deviated from the reported *copA* sequence. We also considered the possibility of RNA editing, where the sequence of the 70th codon would be altered at the mRNA level, but sequencing of the RT-PCR amplified *copA* mRNA showed no difference from the DNA sequence. Having excluded nucleotide sequence alteration as a source of the CopA(Z) C-terminal amino acid change, we explored other scenarios that might lead to the synthesis of a truncated protein with an aberrant amino acid sequence.

Close inspection of the *copA* sequence showed that the GCU70 codon overlaps with a GGC (Gly) codon in the -1 reading frame which, in this alternative frame, is immediately followed by a stop codon (Figure 2A). Furthermore, the triplet GGC appears within the sequence CCCAAAGGC (Figure 2A), which matches the general pattern X-XXY-YYZ that is classified as a 'slippery sequence' (SS) because it has been reported to promote efficient -1 PRF (Jacks et al., 1988a; Sharma et al., 2014). These observations, combined with our experimental data, offer a straightforward explanation for the generation of the CopA(Z) polypeptide ending with a Gly residue. First, ribosomes translating the *copA* ORF undergo -1 PRF within the SS and incorporate a Gly residue instead of an Ala as the 70th amino acid of the polypeptide. Translation then terminates at the following stop codon (Figure 2A) and a short protein with the molecular mass of 9,323 Da, precisely matching the experimentally determined mass of the *in vivo* expressed His_6-CopA(Z), is produced (Figures 1B and 1C).

To verify this scenario, we mutated the SS in the plasmid pCopA from CA**C-CCA-AAG**-GC to CA**T-CCT-AAG**-GC (pCopA-mSS) (Figure 2B). The two introduced mutations preserve the amino acid sequence encoded by the wt *copA* but disrupt the SS and, hence, were expected to prevent the translating ribosome from slipping into the -1 frame. Indeed, Western blot analysis showed that cellular expression of His_6-CopA(Z) (but not of His_6-CopA) was abrogated by the SS mutations (Figure 2B). In addition, we were able to reproduce the PRF event of *copA* in the *E. coli* S30 transcription-translation cell-free system. For this, we generated a DNA template containing the first 94 codons of the gene, which included the SS region ($copA_{1\text{-}282}$ template in Figure 2C). In vitro expression of this template resulted in appearance of the encoded full-length protein ($CopA_{1\text{-}94}$) and of the 70 amino acids long CopA(Z), readily visualized by an SDS gel (Figure 2C). Consistent with our in vivo observations, production of CopA(Z) in the cell free system was abrogated when the SS sequence was altered (Figure 2C). These experimental results provided strong support for the hypothesis that CopA(Z) is generated in vivo and in vitro from the *copA* gene via SS-promoted -1 PRF.

Secondary structure of the *copA* mRNA stimulates -1 PRF

The precipitous drop in ribosome density after the 70th codon of the *copA* gene observed in profiling experiments (Figures 1A) suggests that a large fraction of the ribosomes that initiate translation at the start codon of the gene could shift to the -1 frame and prematurely terminate after translating 70 codons. Because the mere presence of a 7 nucleotide long SS is insufficient to account for PRF (Giedroc et al., 2000), we hypothesized that additional elements residing either in the *copA* mRNA and/or the encoded CopA peptide could stimulate recoding.

The -1 PRF is often promoted by mRNA structural elements that hinder the forward movement of the ribosome along the transcript, thereby stimulating the backwards slippage of the ribosome-tRNA complex (Plant et al., 2003). Computational modeling of the possible folding of the *copA* mRNA segment following the -1 PRF site predicted the formation of a stem-loop structure, which may be a part of a stable pseudoknot (PK) (ΔG = -19.7 kcal/mole) (Figure 3A). Furthermore, the location of the first stem (S1) of the predicted PK relative to the SS is compatible with its stimulatory role in promoting efficient -1 PRF (Giedroc and Cornish, 2009).

We tested the contribution of the downstream mRNA segment containing the putative PK to PRF efficiency by analyzing in vitro expression of CopA(Z) from a series of 3′-truncated *copA* templates (Figure 3B). The longest template, $copA_{1\text{-}312}$, contained the first 104 codons of *copA* (the region encompassing the SS and the entire PK), followed by an engineered stop codon that would direct translation termination in the 0 frame. Expression of this construct yielded both, the full-length encoded protein (104 amino acids-long) and the shorter (70 amino acid-long) CopA(Z) (Figure 3C, lane '1-312'). The -1 PRF efficiency, calculated from the relative intensities of the major products bands, was approximately 45% (Figure 3D). The efficiency of -1 PRF gradually diminished in the progressively 3′-truncated templates in which the second (S2) PK stem (constructs $copA_{1\text{-}261}$ and $copA_{1\text{-}243}$) or both PK stems (construct $copA_{1\text{-}222}$) were eliminated (Figure 3B). CopA(Z) production was largely abrogated when only 15 nucleotides downstream of SS were present in the construct (Figures 3C and 3D). Collectively, the results of these experiments indicate that the mRNA segment downstream of SS likely adopts a specific secondary structure fold and is essential for promoting highly efficient -1 PRF that mediates the generation of CopA(Z).

The CopA nascent peptide modulates -1 PRF

Nascent peptide-ribosome interactions often play an important role in regulation of translation (Ito and Chiba, 2013) and can influence certain recoding events (Chen et al., 2015; Gupta et al., 2013; Samatova et al., 2014; Weiss et al., 1990; Yordanova et al., 2015). We considered the possibility that the CopA nascent chain might affect the frequency of -1 PRF and hence play a role in controlling the relative expression of CopA(Z) and CopA proteins from the same gene. In order to test the effect of the CopA nascent peptide on PRF, we introduced two sets of compensatory single-nucleotide indel mutations within the template $copA_{1\text{-}312}$. The first set of mutations (construct $copA_{1\text{-}312}$-NP1, Figures 4A and S1) altered the sequence of the CopA amino acid residues 4 through 29 located outside of the ribosomal exit tunnel when the ribosome reaches the PRF site (Figures 4A and S1). With

the second set of mutations, the sequence of the CopA segment 31-67, which resides in the exit tunnel of the frameshifting ribosome, was altered (construct *copA*$_{1\text{-}312}$-NP2). The integrity of the SS and the PK regions was preserved in both mutants. Because the amino acid composition of either of the mutant proteins is different from that of the wt CopA(Z), control templates were prepared (constructs CopA(Z)$_M$-NP1 and CopA(Z)$_M$-NP2 in Figure S1) to generate the corresponding mutant CopA(Z) proteins to serve as electrophoretic mobility markers. In vitro -1 PRF efficiencies on the mutant *copA*$_{1\text{-}312}$-NP1 and *copA*$_{1\text{-}312}$-NP2 constructs were calculated from the intensities of the gel bands corresponding to the truncated and full-size products encoded in the 104 codons of the wt and mutant templates. Changing the sequence of the N-terminal segment of CopA (the *copA*$_{1\text{-}312}$-NP1 construct) had little effect on - 1 PRF frequency in vitro, which remained comparable to the wt level (Figures 4B and 4C). However, when the inner-tunnel segment of the CopA nascent chain was altered, PRF efficiency dropped nearly two-fold (Figures 4B and 4C).

We further tested whether the contribution of the nascent peptide to -1 PRF in *copA* is manifested in vivo. For this, we introduced the wt or mutant versions of the *copA*$_{3\text{-}294}$ sequence into the dual luciferase reporter plasmid pEK4 (Grentzmann et al., 1998; Kramer and Farabaugh, 2007) (Figure 4D). In this plasmid, the downstream firefly luciferase (*Fluc*) coding sequence is in the -1 frame relative to the preceding *Renilla* luciferase (*Rluc*) ORF. A -1 PRF is required to generate functional Fluc, whereas Rluc serves as an internal control for the zero-frame translation. Expression of the reporter carrying the wt *copA*$_{3\text{-}294}$ sequence inserted after the *Rluc* ORF resulted in ~32% -1 PRF efficiency (for the purpose of the subsequent comparison, we took the frequency of wt -1 PRF as 100%, Figure 4E). As expected, -1 PRF was abrogated when the slippery sequence was disrupted (mSS reporter in Figure 4, panels D and E). Consistent with the results obtained in vitro, altering the *copA* codons 31-67 in pEK4 to generate the construct NP2 (Figures S1 and 4D) reduced the -1 PRF efficiency by ca. 40% (Figure 4E). We therefore concluded that the CopA nascent chain residing inside the ribosomal exit tunnel modulates the efficiency of -1 PRF during translation of the *copA* gene both in vitro and in vivo.

Diffusible CopA(Z) generated via -1 PRF facilitates cell survival at elevated concentrations of copper

Our experimental data argue that the long-missing enigmatic copper chaperone of *E. coli* is generated via -1 PRF during translation of the *copA* gene. If high-frequency PRF within the *copA* gene is the result of an evolutionary selection rather than a genetic aberrance, production of the diffusible CopA(Z) protein should facilitate the maintenance of copper ion homeostasis. The recent work of Lübben and coworkers has shown that the expression of CopA with an N-terminal truncation, *i. e.*, a version of the transporter protein lacking the MBD1 domain, increased the sensitivity of *E. coli* to copper (Drees et al., 2015). This defect could be rescued by the ectopic expression of the CopA N-terminal protein fragment encompassing MBD1 (Drees et al., 2015), whose identity closely matched the naturally produced CopA(Z) that we observed in our experiments (Figures 1 and 2). Although the result described by Drees et al. hinted that the MBD1 of CopA could possibly function as a metal chaperone, the experimental set-up did not precisely match the true cellular scenario, where CopA(Z) is co-expressed from the *copA* gene via -1 PRF alongside the full-size

CopA transporter. To test whether CopA(Z) contributes to copper tolerance when expressed from the intact *copA* gene, we compared survival of *E. coli* during exposure to copper, when production of the full-size CopA was unaffected but generation of CopA(Z) was either allowed (wt) or prevented by the SS mutations. Two synonymous codon mutations, which disrupted the SS sequence by changing it from CAC_{201}-CCA_{204}-AAG-GC (wt) to $CA\underline{T}_{201}$-$CC\underline{T}_{204}$-AAG-GC (mSS mutant) but did not change the encoded amino acid sequence, were introduced in the *copA* gene of the BW25113 chromosome. We then mixed equal numbers of wt and mSS cells and passaged the culture for several generations at a mildly toxic concentration of $CuSO_4$ (4 mM). Changes in the mSS/wt cell ratio were monitored by PCR-amplifying the *copA* gene from the genomic DNA of the mixed culture and analyzing the Sanger sequencing chromatogram peaks corresponding to the gene's positions 201 and 204, those which differ in the wt and mSS cells (Figure 5, A-C). After 50 generations of growth in the presence of 4 mM $CuSO_4$ most of the cells in the co-culture carried the wt *copA*, whereas the mSS cells had practically disappeared (Figures 5C and 5D). Thus, the production of diffusible CopA(Z) via -1 PRF enables cell survival in the presence of toxic concentrations of copper. This result argues that the presence of PRF signal in the *copA* gene is an evolutionarily selected trait. This conclusion is further supported by the observation that the mRNA structural elements promoting -1 PRF (SS and a predicted PK) are present at the edge of the MBD1-encoding *copA* segment in a wide range of bacterial species (Figures S2 and S3), indicating that co-expression of the copper ion transporter and its chaperone from the same gene could be advantageous for many bacterial species.

A -1 PRF signature could be identified in the human homolog of the bacterial *copA* gene

The transporter protein ATP7B in human cells is homologous to the bacterial CopA and, similar to CopA, catalyzes the efflux of copper ions (Gupta and Lutsenko, 2012). ATP7B carries six MBDs that are involved in copper ion trafficking (Barry et al., 2010; Cater et al., 2004). Interestingly, the heptanucleotide CCCAAAG, identical to the SS of *E. coli copA*, is present between the MBD2- and MBD3-coding segments of *ATP7B* (Figure 6A). Furthermore, the SS in the human gene is immediately followed by an mRNA sequence predicted to form a stable I-type PK (Theis et al., 2008) (ΔG=-27 kcal/mole) (Figure 6B). The arrangement of these elements, which are known to stimulate recoding, suggests that -1 PRF may take place during translation of the *ATP7B* mRNA. Because a stop codon is present in the -1 frame at a short distance after the -1 PRF signal (Figure 6A and 6B), the putative recoding event could result in production of a truncated protein composed of MBD1 and MBD2 of ATP7B.

To assess whether the combination of SS and predicted PK of *ATP7B* could promote -1 PRF, the sequence encompassing these two elements was introduced into a eukaryotic dual luciferase reporter construct (Grentzmann et al., 1998)(Figure 6C) and tested in HEK293T cells. Measuring the relative activities of Rluc and Fluc revealed that the putative recoding elements from the *ATP7B* gene promoted -1 PRF with a 12% efficiency (Figure 6D), a level comparable to that mediated by the well-characterized HIV -1 PRF signal (Jacks et al., 1988b). When a termination codon was introduced prior to the *ATP7B* recoding elements (PTC in Figure 6C) or when a stop codon was inserted at the beginning of the -1 frame *Fluc* ORF (OOF in Figure 6C), the Fluc expression was abrogated, ensuring that expression of

Fluc is indeed driven by PRF that takes place within the *ATP7B*-derived segment of the reporter. A similar arrangement of the SS followed by a putative downstream PK and a stop codon in -1 frame is found in ATP7B homologs of higher primates and some other mammals (Figure S4), an observation that opens the possibility that in these organisms, similar to bacteria, a -1 PRF-based recoding may be involved in generating two *ATP7B*-encoded proteins with related but distinct functions in copper management.

Discussion

While several cases of PRF are known in bacteria (Atkins et al., 2016), there is essentially only one well-substantiated example where -1 PRF leads to generation of two functional proteins from one gene (*dnaX*) (Blinkowa and Walker, 1990). Our finding that -1 PRF in the *E. coli* gene *copA* directs synthesis of two functional proteins illuminates a possible broader penetrance of this distinctive mechanism of protein coding and gene regulation. Several lines of evidence support the view that production of the short CopA(Z) polypeptide along with the full-size CopA from the same gene is a result of evolutionary selection for improved cell fitness, rather than a spontaneous non-consequential genetic aberrance. Firstly, the location of the -1 PRF site is ideal for generating a protein nearly precisely corresponding to the functional MBD1 domain, which, as it has been shown, retains its metal ion binding properties (Drees et al., 2015). Secondly, if spontaneous appearance of a generic heptameric slippery sequence (XXXYYYZ) could be a relatively frequent scenario, its co-occurrence with the mRNA and nascent peptide elements that stimulate PRF should be an extremely rare event. In the case of -1 PRF in *copA*, both the mRNA structure and the specific sequence of the CopA nascent chain contribute to the highly efficient PRF and hence stimulates production of CopA(Z). Thirdly, the conservation of the SS in the *copA* genes of a range of bacterial species together with the presence of a characteristic downstream mRNA structure at a proper distance from the SS to efficiently promote -1 PRF argues that co-production of CopA and its putative diffusible chaperone from one gene is evolutionarily beneficial. The final, but possibly the strongest argument in favor of the functional significance of the *copA* -1 PRF is the fact that abolishing PRF, and thus CopA(Z) production, by SS-disrupting mutations results in reduced cell tolerance to elevated concentrations of copper.

Although exploring the direct function of CopA(Z) in the maintenance of copper homeostasis was beyond the scope of our study, previous reports strongly argue that this protein plays the role of the ‘missing’ copper chaperone in *E. coli*. A recent study has demonstrated that ectopically-expressed MBD1 of CopA can bind copper ions with high affinity and transfer them to the transporter – all characteristics of a metal ion chaperone (Drees et al., 2015). However, because there was no clear evidence that the MBD1 could be naturally produced as an independent protein in *E. coli*, it remained unknown how MBD1 could efficiently scavenge copper ions from the cytoplasm while remaining an integral part of the membrane-embedded transporter. Our finding that CopA MBD1 in fact exists in two forms, transporter-bound and diffusible, solves this conundrum. If this assertion is correct and CopA(Z) is indeed a true ‘free-floating’ copper chaperone, this would make PRF in *copA* a rather unique recoding event, because it leads to the generation of two proteins independently functioning in the same biochemical pathway. This scenario is distinct from

-1 PRF in *dnaX* (Tsuchihashi and Kornberg, 1990) and possibly *csoS2* (Chaijarasphong et al., 2016), where PRF produces two polypeptides of a multi-subunit complex which function as a single enzyme.

One of the intriguing questions about *copA* expression is whether the production of CopA(Z) via -1 PRF occurs with invariable frequency in every growth condition or if, alternatively, the efficiency of PRF and the ratio of CopA(Z) to CopA is subject to regulation. It is conceivable that the formation and/or stability of the downstream mRNA secondary structure could be sensitive to the copper ion concentrations (Furukawa, 2015), or that the PRF-stimulatory effect of the nascent peptide in the ribosomal exit tunnel could be modulated by the metal. Further research is needed to answer these questions.

While the co-occurrence of SS and downstream PK in the *copA* genes of a number of bacterial species strongly suggests that co-expression of a transporter and a putative chaperone is a beneficial trait, the discovery of a similar arrangement of PRF-stimulating elements in the human *ATP7B* gene was unexpected. Until recently, all of the examples of -1 PRF reported for mammalian genomes originate from retroviral insertions (Clark et al., 2007; Manktelow et al., 2005; Wills et al., 2006). However, a recent report revealed the first examples of ‘true’ non-retroviral -1 PRF signals, suggesting that this molecular mechanism is more commonly used than previously thought (Belew et al., 2014). Furthermore, while the SS is present at a short distance after the MBD2-coding segment of the *ATP7B* gene in genomes of several mammals (Figure S4), it is not found in many other eukaryotes. At this point we do not have clear evidence whether -1 PRF indeed occurs in the human *ATP7B* gene or results in the production of a truncated protein with chaperone or other auxiliary functions in maintaining copper homeostasis. However, the fact that the *ATP7B*-derived element directs efficient in vivo -1 PRF in the luciferase reporter is compatible with such a scenario. Mutations in the *ATP7B* gene resulting in impairment of copper excretion have been linked to Wilson disease (Bull et al., 1993). It is worthwhile exploring whether some of the mutations, which cause the disease, could disrupt production of not only the ATP7B-encoded transporter protein, but also of the functional shorter polypeptide.

Contact for Reagent and Resource Sharing

Further information and requests for reagents may be directed to, and will be fulfilled by the corresponding author, Dr. Alexander Mankin (shura@uic.edu).

Method Details

Strains and plasmids

The ASKA collection plasmid that we named pCopA carries the *E. coli copA* gene encoding the N-terminally His_6-tagged CopA protein (Kitagawa et al., 2005). The pCopA plasmid was introduced into the Keio collection *E. coli* strain JW0473-3 lacking chromosomal *copA* (*copA::kan*) (Baba et al., 2006). The point mutations that generated the PRF-deficient *copA* variant in the pCopA-mSS plasmid were engineered using the QuikChange Lightning Multi Site-Directed Mutagenesis kit (Agilent Technologies) and the primer #1 (all primer sequences are listed in Table S1). The PRF-deficient variant of the chromosomal *copA*

(mSS), in which the SS sequence CA**C**$_{201}$**-CCA**$_{204}$**-AAG**-GC was mutated to CA**T**$_{201}$**-CCT**$_{204}$**-AAG**-GC, was engineered in the BW25113 strain by homologous recombination using the pKOV plasmid (Link et al., 1997). Two PCR products were generated: Primers #11 and #12 were used to generate the first one, using plasmid pCopA-mSS as the template; primers #13 and #14 were used to prepare the second product using genomic DNA of *E. coli* BW25113 as the template. Both PCR products, which contain overlapping sequences, were introduced by Gibson assembly into the pKOV plasmid cut with NotI and BamHI restriction enzymes. The resulting pKOV-mSS plasmid, carrying the sequence starting 800 nucleotides upstream and ending 1207 nucleotides downstream from the start codon of the mutant *copA* gene, was transformed into BW25113 cells by electroporation. The transformants were plated onto LB/agar supplemented with 30 μg/mL of chloramphenicol and plates were incubated overnight at 42°C to induce integration of the plasmid into the chromosome. Several colonies were resuspended in 1 mL LB and dilutions were plated on LB agar plates supplemented with 5% (w/v) sucrose to induce resolution of the vector. After overnight incubation of the plates at 37°C, the loss of the vector plasmid was confirmed by replica plating which showed the sensitivity of the cells to chloramphenicol. The resulting strain mSS was used in the competition experiments. The bacterial dual luciferase reporter plasm ids were prepared on the basis of the pEK4 plasmid (Grentzmann et al., 1998; Kramer and Farabaugh, 2007). To engineer the reporter plasmids with the *copA* -1 PRF element, three PCR fragments (DLR1, DLR2 and DLR3) were generated using plasmid pCopA as the template. The PCR products DLR1 (primers #15 and #16), DLR2 (primers #17 and #18), and DLR3 (primers #19 and #20), that contain overlapping sequences, were introduced by Gibson assembly into pEK4 cut with SalI/SacI to generate pEK4-*copA*$_{3\text{-}294}$-wt. The resulting plasmid contained codons 2 to 98 of the wt *copA* inserted in frame after the first (Rluc) gene in pEK4. Similarly, pEK4-*copA*$_{3\text{-}294}$-mSS was assembled from the same DLR1, DLR3 fragments and the DLR2-mSS PCR product, which was amplified from the pCopA-mSS plasmid using primers #21 and #22. Plasmid pEK4-*copA*$_{3\text{-}294}$-NP2 was assembled from the DLR3 fragment combined with DLR1-NP2 and DLR2-NP2 amplified from the synthetic *copA*$_{1\text{-}312}$-NP2 gBlock (Table S1) using primers #15 and #16 or primers #23 and #24, respectively. In all three reporter plasmids, the *copA* sequence carried the deletion of nucleotide T210, located downstream of the entire -1 PRF signal, introduced to eliminate an in-frame stop codon and allowed for translation of the *Fluc* ORF upon -1 PRF. Control plasmid pEK4-*copA*$_{3\text{-}294}$-C, which was used for normalization of the relative levels of Rluc and Fluc expression in the absence of -1 PRF, contained *Fluc* and *Rluc* in the 0 frame, whereas the *copA* -1 PRF was disabled by the mSS mutations. This plasmid was obtained by introducing the DLR-C fragment, amplified from pCopA-mSS using primers #25 and #26, into the SalI/SacI cut pEK4 plasmid. The 0-frame version of pEK4-*copA*$_{3\text{-}294}$-NP2-C control plasmid was constructed using fragments DLR1-NP2, DLR2-NP2-C (primers #27 and #28) and DLR3-NP2-C (primers #19 and #29), which were introduced into SalI/SacI cut pEK4 by Gibson assembly. The Gibson assembly reactions were transformed into *E. coli* JM109 cells. Plasmids with the desired sequences were then introduced into BW25113 host cells in order to carry out the dual luciferase reporter assays.

Overexpression of *copA* and purification of CopA(Z)

The *E. coli* Δ*copA* cells (JW0473-3) carrying the pCopA plasmid were grown at 37°C in LB medium supplemented with kanamycin (50 μg/mL) and chloramphenicol (30 μg/mL). Upon reaching an A_{600} of 0.6, cultures were induced with 0.1 mM isopropyl-β-D-1-thiogalactopyranoside (IPTG) and incubation continued for 3 hours. Cells were collected by centrifugation at 4°C, resuspended in buffer 20 mM Tris pH 8.0, 300 mM NaCl, 30 mM imidazole supplemented with 1× Halt Protease Inhibitor (Life Technologies) and lysed using a French Press at 16,000 psi. The lysate was clarified by centrifugation at 15,000 rpm (rotor JA-25.50) for 1 hour at 4°C and then filtered through a 0.2 μm cellulose acetate filter. The lysate was passed through a HisTrap HP column (GE) using an AKTA/Unicorn FPLC system (GE). Bound protein was eluted using a linear 30-300 mM imidazole gradient. Fractions in which the CopA(Z) protein was detected, as assessed by SDS gel electrophoresis [4-20% TGX (Bio-Rad)], were pooled together and subjected to an additional round of purification on the HisTrap HPcolumn, this time using a step-wise 30-300 mM imidazole elution. The purified protein was dialyzed using Spectra/Por membrane (MWCO 3,500) against 10 mM ammonium acetate pH 8.0 for 3 h at 4°C. The recovered sample was concentrated in Amicon concentrator (MWCO 3,000). Concentration of the isolated protein was measured using the bicinchoninic acid assay (BCA) kit (Thermo Scientific) and its purity was confirmed by gel electrophoresis and silver staining (Chevallet et al., 2006).

Mass spectrometry analysis

Purified protein (~100 μg) was precipitated with cold acetone to remove salts and re-suspended in 4% SDS prior to the addition of GELFREE loading buffer. Separation was performed as described (Tran and Doucette, 2009) using a 10% gel on a commercial GELFREE 8100 system (Expedeon, Cambridge, UK). The fraction containing CopA(Z) was isolated and SDS was removed using the methanol-chloroform-water method (Wessel and Flugge, 1984). After SDS removal, proteins were resuspended in 40 μL solvent A (94.9% H_2O, 5% acetonitrile, 0.1% formic acid) and 5 μL were injected onto a trap column (150 μm ID × 3 cm) coupled with a nanobore analytical column (75 μm ID × 15 cm). The trap and analytical column were packed with polymeric reverse phase media (5 μm, 1,000 Å pore size) (PLRPS, Phenomenex). Samples were separated using a linear gradient of solvent A and solvent B (4.9% water, 95% acetonitrile, 0.1% formic acid) over 60 minutes. MS data were obtained on an Orbitrap Elite mass spectrometer (Thermo Scientific) fitted with a custom nanospray ionization source. Intact mass spectrometry data were obtained at a resolving power of 120,000 (m/z 400). The top 2 m/z species were isolated within the Velos ion trap and fragmented using higher energy collisional dissociation (HCD). Data were analyzed with ProSightPC against a custom CopA database.

Western blotting

Five micrograms of total protein from lysates of uninduced or IPTG-induced BW25113 cells transformed with pCopA or pCopA-mSS were loaded on a 4-20% polyacrylamide-SDS gel (TGX, Bio-Rad). Resolved proteins were transferred to a PVDF membrane (Bio-Rad) by electroblotting (Bio-Rad Trans-blot SD Semi-Dry Transfer Cell, 10 min at 25 V). The

membrane was blocked with 3% BSA (Sigma-Aldrich) in TBST buffer (10 mM Tris-Cl pH 7.4; 150 mM NaCl, 0.1% Tween-20) and probed with 6×-His Epitope Tag Antibody HRP conjugate (Thermo Scientific) at 1:2000 dilution. The blots were developed using Clarity™ Western ECL substrate (BioRad) and visualized using FluorChem™ R System (Protein Simple).

Growth competition experiments

Overnight cultures of wt (BW25113) and mSS cells were diluted 1:100 in fresh LB and grown to mid-log phase (A_{600} ~ 0.5). The cell densities in both cultures were adjusted to the same value and equal volumes of the wt and mSS cultures were mixed. The 1:1 cell mixture (starting culture) was diluted to A_{600} of 0.001 and grown overnight in LB without or with the addition of 4 mM $CuSO_4$. Five microliters of the overnight culture was diluted into 5 mL LB without or with 4 mM $CuSO_4$. Cultures were diluted 1000-fold upon reaching saturation for a total of 5 passages. Aliquots from every passage were used to isolate genomic DNA and the SS region of *copA* was PCR amplified using primers #6 and #11 (Table S1) and the following PCR conditions: 94°C, 2 min followed by 34 cycles 94°C, 2 min; 52°C, 30 sec; 68°C, 15 sec, and final extension at 68°C for 2 min. The PCR fragments were subjected to Sanger sequencing using primer #6. The ratio of the mSS to wt cells was estimated by quantifying and then averaging the heights of the sequencing chromatogram peaks corresponding to *copA* residues 201 (C for wt, T for mSS) and 204 (C for wt, T for mSS).

In vitro measurement of -1 PRF efficiency

Coupled in vitro transcription-translation reactions in the *E. coli* lysate were performed using a S30 transcription-translation system for linear DNA (Promega). DNA templates (0.6 pmol) were PCR-amplified from either *E. coli* BW25113 genomic DNA or the plasmid pCopA-mSS (using primers #2 to #10 for both), or from synthetic gBlocks (Table S1). The resulting templates carrying the gene segment of interest controlled by the P*trc* promoter were translated in 5 μL reactions containing 2 μCi of [^{35}S]-L-methionine (specific activity 1175 Ci/mmol) (MP Biomedicals). Reactions were incubated at 37°C for 30 minutes and translation products were precipitated with 8 volumes of cold acetone. After the recovery of the pellet by centrifugation, proteins were resolved on 16.5% Tricine-SDS polyacrylamide gels (Schägger and von Jagow, 1987). The gels were dried, exposed to a phosphorimager screen, and visualized with a Typhoon scanner (GE). Protein bands corresponding to CopA(Z) (the -1 PRF product) and the relevant truncated CopA reference (originated from 0-frame translation) were quantified using the ImageJ software (http://rsbweb.nih.gov/ij/). PRF efficiency was estimated as a ratio of the density of the CopA(Z) band to the combined density of CopA(Z) and full-protein gel bands.

Identification of -1 PRF elements in different species

Bacterial orthologs of *copA* (*E. coli*) were retrieved from OrthologueDB (Waterhouse et al., 2013). Coordinates of metal binding domains (MBD) of CopA were determined by HMMSEARCH and Pfam model PF00403 (Finn et al., 2014; Wistrand and Sonnhammer, 2005). For prediction of -1 PRF elements analogous to -1 PRF signal in the *E. coli copA*, the bacterial *copA* genes encoding 2 sequential MBDs were selected. The gene segments separating two MBDs were scanned for the presence of -1 PRF signals (-1 frame slippery

sequence, nearby -1 frame stop codon and a downstream mRNA structure) using KnotInFrame (Theis et al., 2008). For the genes with the interdomain-coding segment shorter than 50 nt, the last 50 nt of the MBD1 coding sequence and the first 150 nt of the MBD2 coding sequence were also included in the KnotInFrame search. After removing redundancy for the strains of the same species, the predicted -1 PRF is found in 35 *copA* genes belonging primarily to the proteobacteria branch of the bacterial phylogenetic tree. Maximum Likelihood (ML) tree for 35 CopA sequences was computed (Huerta-Cepas et al., 2016) and the resultant tree (Figure S2) was decorated with phyla/class level taxonomy information. The structure of *copA* mRNA was initially modeled by using IPknot (Sato et al., 2011) and KnotInFrame (Theis et al., 2008). The Simulfold program (Meyer and Miklos, 2007) was used to generate the final consensus structure and the covariational mutations (Figures 3 and S3). Aligned cDNA sequences of human ATP7B and its orthologs (Figure S4) were retrieved from Ensembl (release 85) (Aken et al., 2016). The prediction of *ATP7B* mRNA downstream structure was based on KnotInFrame (Theis et al., 2008) by submitting downstream 100 nt-long sequence as input.

Bacterial dual luciferase reporter assay

The *E. coli* BW25113 cells carrying the derivatives of the pEK4 plasmid were grown at 37°C in 5 mL LB medium supplemented with 50 μg/mL of ampicillin. Upon reaching A_{600} of 0.5, cells were collected by centrifugation at 4°C and then resuspended in 200 μL of Lysis Buffer (1 mg/mL lysozyme, 10 mM Tris-HCl pH 8.0, 1 mM EDTA). The lysates were prepared by freezing-thawing as previously described (de Wet et al., 1985). Five microliters of the extracts were used for F-luc and R-luc activities using the Dual-Luciferase® Reporter Assay System (Promega). Luminescence was measured in 96-well plates in Top Count NXT (Perkin Elmer). The PRF efficiency (ρPRF) was calculated using the equation: $\rho PRF = (Fluc_{test}/Rluc_{test})/(Fluc_{control}/Rluc_{control})$ (Grentzmann et al., 1998), where test plasmids were pEK4-*copA*$_{3\text{-}294}$, pEK4-*copA*$_{3\text{-}294}$-mSS and pEK4-*copA*$_{3\text{-}294}$-NP2; the control plasmids were pEK4-*copA*$_{3\text{-}294}$-C and pEK4-*copA*$_{3\text{-}294}$-NP2-C, as described in Star Methods. Experimental replicates were performed using lysates prepared from bacterial cultures grown from three independent colonies.

Dual luciferase assay for -1 PRF in human cells

The *ATP7B*-derived sequence indicated in Figure 6B, acquired as a gBlock (Integrated DNA Technologies) (Table S1, #32-34), was cloned into SalI/SacI cut p2luci plasmid so that a -1 PRF event would direct ribosomes elongating through the upstream Rluc ORF into the downstream Fluc ORF. Two additional mutants, one harboring a UAA termination codon in the 0-frame immediately 5′ of the *ATP7B*-derived sequence, and the other with a termination codon in the -1 frame 3′ of the *ATP7B*-derived sequence were also constructed on the basis of this vector. Plasmid constructs verified by DNA sequencing were transfected into HEK293T human cells. The dual luciferase assays were performed as previously described (Harger and Dinman, 2003) and the resulting data reflecting relative activity of the expressed Fluc and Rluc proteins were subjected to statistical analyses (Jacobs and Dinman, 2004). Assays were repeated at least 5 times until statistical significance was achieved.

Supplementary Material

Refer to Web version on PubMed Central for supplementary material.

Acknowledgments

We thank Pavel Baranov and John Atkins for helpful advice, Kurt Fredrick and Hyunwoo Lee for providing the pEK4 and pKOV plasmids, respectively, Andrew Jin for help with some experiments, Dimple Modi, Nikolay Aleksashin and Hao Lei for advice with some experimental procedures. This work was supported by the grants MCB 1244455 and MCB 1615851 (both to A.S.M. and N.V.-L.) from the National Science Foundation and R01 GM117177 and R01HL119439-01A1 (to J.D.D.) from the National Institutes of Health. Proteomics analysis was performed at the Northwestern Proteomics Core Facility supported by the grants NCI CCSG P30 CA060553 and P41 GM108569 from the National Institutes of Health.

References

Aken BL, Ayling S, Barrell D, Clarke L, Curwen V, Fairley S, Fernandez Banet J, Billis K, Garcia Giron C, Hourlier T, et al. The Ensembl gene annotation system. Database (Oxford). 2016; baw093

Arredondo M, Nunez MT. Iron and copper metabolism. Mol Aspects Med. 2005; 26:313–327. [PubMed: 16112186]

Atkins JF, Loughran G, Bhatt PR, Firth AE, Baranov PV. Ribosomal frameshifting and transcriptional slippage: From genetic steganography and cryptography to adventitious use. Nucleic Acids Res. 2016; 44:7007–7078. [PubMed: 27436286]

Baba T, Ara T, Hasegawa M, Takai Y, Okumura Y, Baba M, Datsenko KA, Tomita M, Wanner BL, Mori H. Construction of Escherichia coli K-12 in-frame, single-gene knockout mutants: the Keio collection. Mol Syst Biol. 2006; 2 20060008.

Balakrishnan R, Oman K, Shoji S, Bundschuh R, Fredrick K. The conserved GTPase LepA contributes mainly to translation initiation in Escherichia coli. Nucleic Acids Res. 2014; 42:13370–13383. [PubMed: 25378333]

Banci L, Bertini I, Del Conte R, Markey J, Ruiz-Duenas FJ. Copper trafficking: the solution structure of Bacillus subtilis CopZ. Biochemistry. 2001; 40:15660–15668. [PubMed: 11747441]

Baranov PV, Gesteland RF, Atkins JF. Recoding: translational bifurcations in gene expression. Gene. 2002; 286:187–201. [PubMed: 11943474]

Barry AN, Shinde U, Lutsenko S. Structural organization of human Cu-transporting ATPases: learning from building blocks. J Biol Inorg Chem. 2010; 15:47–59. [PubMed: 19851794]

Belew AT, Meskauskas A, Musalgaonkar S, Advani VM, Sulima SO, Kasprzak WK, Shapiro BA, Dinman JD. Ribosomal frameshifting in the CCR5 mRNA is regulated by miRNAs and the NMD pathway. Nature. 2014; 512:265–269. [PubMed: 25043019]

Blinkowa AL, Walker JR. Programmed ribosomal frameshifting generates the Escherichia coli DNA polymerase III gamma subunit from within the tau subunit reading frame. Nucleic Acids Res. 1990; 18:1725–1729. [PubMed: 2186364]

Bull PC, Thomas GR, Rommens JM, Forbes JR, Cox DW. The Wilson disease gene is a putative copper transporting P-type ATPase similar to the Menkes gene. Nat Genet. 1993; 5:327–337. [PubMed: 8298639]

Caliskan N, Peske F, Rodnina MV. Changed in translation: mRNA recoding by -1 programmed ribosomal frameshifting. Trends Biochem Sci. 2015; 40:265–274. [PubMed: 25850333]

Cater MA, Forbes J, La Fontaine S, Cox D, Mercer JF. Intracellular trafficking of the human Wilson protein: the role of the six N-terminal metal-binding sites. Biochem J. 2004; 380:805–813. [PubMed: 14998371]

Chaijarasphong T, Nichols RJ, Kortright KE, Nixon CF, Teng PK, Oltrogge LM, Savage DF. Programmed ribosomal frameshifting mediates expression of the alpha-carboxysome. J Mol Biol. 2016; 428:153–164. [PubMed: 26608811]

Chen J, Coakley A, O'Connor M, Petrov A, O'Leary SE, Atkins JF, Puglisi JD. Coupling of mRNA structure rearrangement to ribosome movement during bypassing of non-coding regions. Cell. 2015; 163:1267–1280. [PubMed: 26590426]

Chevallet M, Luche S, Rabilloud T. Silver staining of proteins in polyacrylamide gels. Nat Protoc. 2006; 1:1852–1858. [PubMed: 17487168]

Clark MB, Janicke M, Gottesbuhren U, Kleffmann T, Legge M, Poole ES, Tate WP. Mammalian gene PEG10 expresses two reading frames by high efficiency -1 frameshifting in embryonic-associated tissues. J Biol Chem. 2007; 282:37359–37369. [PubMed: 17942406]

Cobine P, Wickramasinghe WA, Harrison MD, Weber T, Solioz M, Dameron CT. The Enterococcus hirae copper chaperone CopZ delivers copper(I) to the CopY repressor. FEBS Lett. 1999; 445:27–30. [PubMed: 10069368]

Craigen WJ, Caskey CT. Expression of peptide chain release factor 2 requires high-efficiency frameshift. Nature. 1986; 322:273–275. [PubMed: 3736654]

de Wet JR, Wood KV, Helinski DR, DeLuca M. Cloning of firefly luciferase cDNA and the expression of active luciferase in Escherichia coli. Proc Natl Acad Sci U S A. 1985; 82:7870–7873. [PubMed: 3906652]

Drees SL, Beyer DF, Lenders-Lomscher C, Lubben M. Distinct functions of serial metal-binding domains in the Escherichia coli P1 B -ATPase CopA. Mol Microbiol. 2015; 97:423–438. [PubMed: 25899340]

Elgamal S, Katz A, Hersch SJ, Newsom D, White P, Navarre WW, Ibba M. EF-P dependent pauses integrate proximal and distal signals during translation. PLoS Genet. 2014; 10:e1004553. [PubMed: 25144653]

Fan B, Grass G, Rensing C, Rosen BP. Escherichia coli CopA N-terminal Cys(X)(2)Cys motifs are not required for copper resistance or transport. Biochem Biophys Res Commun. 2001; 286:414–418. [PubMed: 11500054]

Fan B, Rosen BP. Biochemical characterization of CopA, the Escherichia coli Cu(I)-translocating P-type ATPase. J Biol Chem. 2002; 277:46987–46992. [PubMed: 12351646]

Farabaugh PJ. Programmed translational frameshifting. Annu Rev Genet. 1996; 30:507–528. [PubMed: 8982463]

Farabaugh PJ, Bjork GR. How translational accuracy influences reading frame maintenance. EMBO J. 1999; 18:1427–1434. [PubMed: 10075915]

Finn RD, Bateman A, Clements J, Coggill P, Eberhardt RY, Eddy SR, Heger A, Hetherington K, Holm L, Mistry J, et al. Pfam: the protein families database. Nucleic Acids Res. 2014; 42:D222–230. [PubMed: 24288371]

Flower AM, McHenry CS. The gamma subunit of DNA polymerase III holoenzyme of Escherichia coli is produced by ribosomal frameshifting. Proc Natl Acad Sci U S A. 1990; 87:3713–3717. [PubMed: 2187190]

Furukawa K, Ramesh A, Zhou Z, Weinberg Z, Vallery T, Winkler WC, Breaker RR. Bacterial riboswitches cooperatively bind ni(2+) or co(2+) ions and control expression of heavy metal transporters. Mol Cell. 2015; 57:1088–1098. [PubMed: 25794617]

Giedroc DP, Cornish PV. Frameshifting RNA pseudoknots: structure and mechanism. Virus Res. 2009; 139:193–208. [PubMed: 18621088]

Giedroc DP, Theimer CA, Nixon PL. Structure, stability and function of RNA pseudoknots involved in stimulating ribosomal frameshifting. J Mol Biol. 2000; 298:167–185. [PubMed: 10764589]

Grentzmann G, Ingram JA, Kelly PJ, Gesteland RF, Atkins JF. A dual-luciferase reporter system for studying recoding signals. RNA. 1998; 4:479–486. [PubMed: 9630253]

Guo MS, Updegrove TB, Gogol EB, Shabalina SA, Gross CA, Storz G. MicL, a new sigmaE-dependent sRNA, combats envelope stress by repressing synthesis of Lpp, the major outer membrane lipoprotein. Genes Dev. 2014; 28:1620–1634. [PubMed: 25030700]

Gupta A, Lutsenko S. Evolution of copper transporting ATPases in eukaryotic organisms. Curr Genomics. 2012; 13:124–133. [PubMed: 23024604]

Gupta P, Kannan K, Mankin AS, Vazquez-Laslop N. Regulation of gene expression by macrolide-induced ribosomal frameshifting. Mol Cell. 2013; 52:629–642. [PubMed: 24239289]

Harger JW, Dinman JD. An in vivo dual-luciferase assay system for studying translational recoding in the yeast Saccharomyces cerevisiae. RNA. 2003; 9:1019–1024. [PubMed: 12869712]

Huerta-Cepas J, Serra F, Bork P. ETE 3: reconstruction, analysis, and visualization of phylogenomic Data. Mol Biol Evol. 2016; 33:1635–1638. [PubMed: 26921390]

Ito K, Chiba S. Arrest peptides: cis-acting modulators of translation. Annu Rev Biochem. 2013; 82:171–202. [PubMed: 23746254]

Jacks T, Madhani HD, Masiarz FR, Varmus HE. Signals for ribosomal frameshifting in the Rous sarcoma virus gag-pol region. Cell. 1988a; 55:447–458. [PubMed: 2846182]

Jacks T, Power MD, Masiarz FR, Luciw PA, Barr PJ, Varmus HE. Characterization of ribosomal frameshifting in HIV-1 gag-pol expression. Nature. 1988b; 331:280–283. [PubMed: 2447506]

Jacobs JL, Dinman JD. Systematic analysis of bicistronic reporter assay data. Nucleic Acids Res. 2004; 32:e160. [PubMed: 15561995]

Jordan IK, Natale DA, Koonin EV, Galperin MY. Independent evolution of heavy metal-associated domains in copper chaperones and copper-transporting atpases. J Mol Evol. 2001; 53:622–633. [PubMed: 11677622]

Kannan K, Kanabar P, Schryer D, Florin T, Oh E, Bahroos N, Tenson T, Weissman JS, Mankin AS. The general mode of translation inhibition by macrolide antibiotics. Proc Natl Acad Sci U S A. 2014; 111:15958–15963. [PubMed: 25349425]

Kitagawa M, Ara T, Arifuzzaman M, Ioka-Nakamichi T, Inamoto E, Toyonaga H, Mori H. Complete set of ORF clones of Escherichia coli ASKA library (a complete set of E. coli K-12 ORF archive): unique resources for biological research. DNA Res. 2005; 12:291–299. [PubMed: 16769691]

Kramer EB, Farabaugh PJ. The frequency of translational misreading errors in E. coli is largely determined by tRNA competition. RNA. 2007; 13:87–96. [PubMed: 17095544]

Kurland CG. Translational accuracy and the fitness of bacteria. Annu Rev Genet. 1992; 26:29–50. [PubMed: 1482115]

Li GW, Burkhardt D, Gross C, Weissman JS. Quantifying absolute protein synthesis rates reveals principles underlying allocation of cellular resources. Cell. 2014; 157:624–635. [PubMed: 24766808]

Link AJ, Phillips D, Church GM. Methods for generating precise deletions and insertions in the genome of wild-type Escherichia coli: application to open reading frame characterization. J Bacteriol. 1997; 179:6228–6237. [PubMed: 9335267]

Manktelow E, Shigemoto K, Brierley I. Characterization of the frameshift signal of Edr, a mammalian example of programmed -1 ribosomal frameshifting. Nucleic Acids Res. 2005; 33:1553–1563. [PubMed: 15767280]

Meyer IM, Miklos I. SimulFold: simultaneously inferring RNA structures including pseudoknots, alignments, and trees using a Bayesian MCMC framework. PLoS Comput Biol. 2007; 3:e149. [PubMed: 17696604]

Migocka M. Copper-transporting ATPases: The evolutionarily conserved machineries for balancing copper in living systems. IUBMB Life. 2015; 67:737–745. [PubMed: 26422816]

Mohammad F, Woolstenhulme CJ, Green R, Buskirk AR. Clarifying the translational pausing landscape in bacteria by ribosome profiling. Cell Rep. 2016; 14:686–694. [PubMed: 26776510]

Oh E, Becker AH, Sandikci A, Huber D, Chaba R, Gloge F, Nichols RJ, Typas A, Gross CA, Kramer G, et al. Selective ribosome profiling reveals the cotranslational chaperone action of trigger factor in vivo. Cell. 2011; 147:1295–1308. [PubMed: 22153074]

Outten CE, O'Halloran TV. Femtomolar sensitivity of metalloregulatory proteins controlling zinc homeostasis. Science. 2001; 292:2488–2492. [PubMed: 11397910]

Palumaa P. Copper chaperones. The concept of conformational control in the metabolism of copper. FEBS Lett. 2013; 587:1902–1910. [PubMed: 23684646]

Percival SS, Kauwell GP, Bowser E, Wagner M. Altered copper status in adult men with cystic fibrosis. J Am Coll Nutr. 1999; 18:614–619. [PubMed: 10613413]

Plant EP, Jacobs KL, Harger JW, Meskauskas A, Jacobs JL, Baxter JL, Petrov AN, Dinman JD. The 9-A solution: how mRNA pseudoknots promote efficient programmed -1 ribosomal frameshifting. RNA. 2003; 9:168–174. [PubMed: 12554858]

Rensing C, Fan B, Sharma R, Mitra B, Rosen BP. CopA: an Escherichia coli Cu(I)-translocating P-type ATPase. Proc Natl Acad Sci U S A. 2000; 97:652–656. [PubMed: 10639134]

Rensing C, Grass G. Escherichia coli mechanisms of copper homeostasis in a changing environment. FEMS Microbiol Rev. 2003; 27:197–213. [PubMed: 12829268]

Samatova E, Konevega AL, Wills NM, Atkins JF, Rodnina MV. High-efficiency translational bypassing of non-coding nucleotides specified by mRNA structure and nascent peptide. Nat Commun. 2014; 5:4459. [PubMed: 25041899]

Sato K, Kato Y, Hamada M, Akutsu T, Asai K. IPknot: fast and accurate prediction of RNA secondary structures with pseudoknots using integer programming. Bioinformatics. 2011; 27:i85–93. [PubMed: 21685106]

Schägger H, von Jagow G. Tricine-sodium dodecyl sulfate-polyacrylamide gel electrophoresis for the separation of proteins in the range from 1 to 100 kDa. Anal Biochem. 1987; 166:368–379. [PubMed: 2449095]

Schneider CA, Rasband WS, Eliceiri KW. NIH Image to ImageJ: 25 years of image analysis. Nat Methods. 9:671–675. 2012.

Sharma V, Prere MF, Canal I, Firth AE, Atkins JF, Baranov PV, Fayet O. Analysis of tetra- and hepta-nucleotides motifs promoting -1 ribosomal frameshifting in Escherichia coli. Nucleic Acids Res. 2014; 42:7210–7225. [PubMed: 24875478]

Theis C, Reeder J, Giegerich R. KnotInFrame: prediction of -1 ribosomal frameshift events. Nucleic Acids Res. 2008; 36:6013–6020. [PubMed: 18820303]

Torsdottir G, Kristinsson J, Sveinbjornsdottir S, Snaedal J, Johannesson T. Copper, ceruloplasmin, superoxide dismutase and iron parameters in Parkinson's disease. Pharmacol Toxicol. 1999; 85:239–243. [PubMed: 10608487]

Tran JC, Doucette AA. Multiplexed size separation of intact proteins in solution phase for mass spectrometry. Anal Chem. 2009; 81:6201–6209. [PubMed: 19572727]

Tsuchihashi Z, Kornberg A. Translational frameshifting generates the gamma subunit of DNA polymerase III holoenzyme. Proc Natl Acad Sci U S A. 1990; 87:2516–2520. [PubMed: 2181440]

Vulpe C, Levinson B, Whitney S, Packman S, Gitschier J. Isolation of a candidate gene for Menkes disease and evidence that it encodes a copper-transporting ATPase. Nat Genet. 1993; 3:7–13. [PubMed: 8490659]

Wasinger VC, Humphery-Smith I. Small genes/gene-products in Escherichia coli K-12. FEMS Microbiol Lett. 1998; 169:375–382. [PubMed: 9868784]

Waterhouse RM, Tegenfeldt F, Li J, Zdobnov EM, Kriventseva EV. OrthoDB: a hierarchical catalog of animal, fungal and bacterial orthologs. Nucleic Acids Res. 2013; 41:D358–365. [PubMed: 23180791]

Weiss RB, Dunn DM, Atkins JF, Gesteland RF. Ribosomal frameshifting from -2 to +50 nucleotides. Prog Nucleic Acid Res Mol Biol. 1990; 39:159–183. [PubMed: 2247607]

Wessel D, Flugge UI. A method for the quantitative recovery of protein in dilute solution in the presence of detergents and lipids. Anal Biochem. 1984; 138:141–143. [PubMed: 6731838]

Wills NM, Moore B, Hammer A, Gesteland RF, Atkins JF. A functional -1 ribosomal frameshift signal in the human paraneoplastic Ma3 gene. J Biol Chem. 2006; 281:7082–7088. [PubMed: 16407312]

Wistrand M, Sonnhammer EL. Improved profile HMM performance by assessment of critical algorithmic features in SAM and HMMER. BMC Bioinformatics. 2005; 6:99. [PubMed: 15831105]

Yordanova MM, Wu C, Andreev DE, Sachs MS, Atkins JF. A nascent peptide signal responsive to endogenous levels of polyamines acts to stimulate regulatory frameshifting on antizyme mRNA. J Biol Chem. 2015; 290:17863–17878. [PubMed: 25998126]

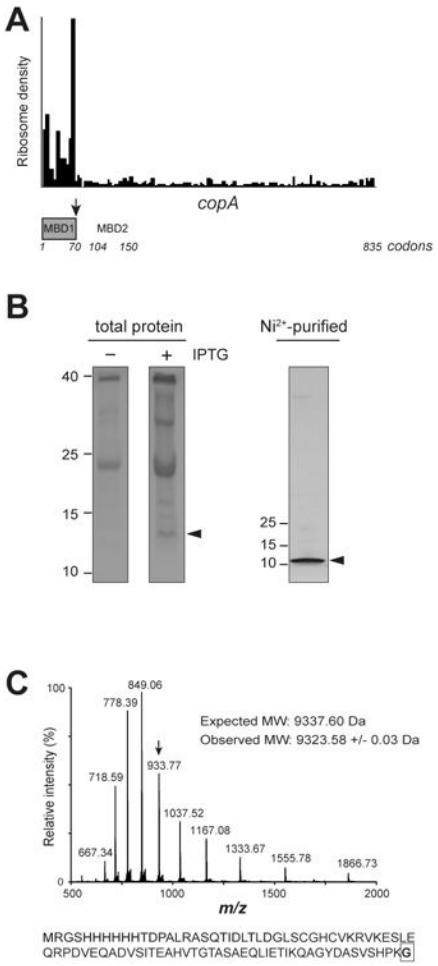

Figure 1. The short polypeptide CopA(Z) is translated in the cell from the *E. coli copA* gene

(A) Ribosome profiling reveals an abrupt drop in ribosome density around the 70th codon of the *copA* gene (black arrow). The boundaries of the two metal binding domains MBD1 and MBD2 of the CopA transporter protein encoded in the *copA* gene are indicated; MBD1 is colored grey. The profiling data are from the control cells in (Kannan et al., 2014).

(B) Two left panels: Coomassie-stained 15% SDS gel showing low-molecular weight proteins in the control and IPTG-induced Δ*copA E. coli* cells carrying the pCopA plasmid which encodes N-terminally His_6-tagged CopA. Right: silver-stained 4-20% SDS gel showing the N-terminally His_6-tagged short protein expressed in the IPTG-induced cells and purified by Ni^{2+}-affinity chromatography. The short protein with the electrophoretic mobility approximately corresponding to the His_6-tagged MBD1 of CopA, that we named CopA(Z), is indicated by arrowheads.

(C) Top-down mass-spectrometric analysis of the purified His_6-tagged CopA(Z). The deconvoluted monoisotopic mass of 9323.61 Da is consistent with the predicted mass of CopA(Z) (9337.60 Da), where the C-terminal Ala, encoded in the 70th codon of *copA*, is replaced with Gly. The spectrum shows multiply charged species of the intact protein; for reference, the peak corresponding to the charge 10+ is indicated by an arrow for reference. The amino acid sequence of His_6-tagged CopA(Z) is shown below and the C-terminal Gly is boxed.

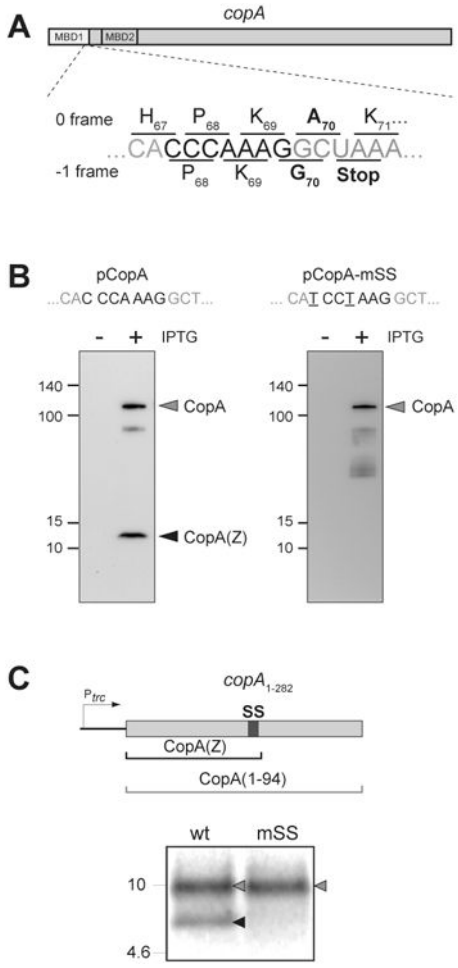

Figure 2. Production of CopA(Z) depends on the integrity of the slippery sequence present in the *copA* gene

(A) The slippery sequence CCCAAAG present in the *copA* gene at the end of the MBD1-coding segment. Slippage of the ribosome to the -1 frame would cause the ribosome to incorporate Gly-70 after Lys-69 and terminate translation at the following stop codon, generating the CopA(Z) protein.

(B) Immunoblot of the lysates of *E. coli* cells carrying either the pCopA plasmid containing the wt *copA* gene, or pCopA-mSS in which the slippery sequence was mutated to prevent -1 PRF. The CopA (grey arrowhead) and CopA(Z) (black arrowhead) proteins were detected using anti-His_6-tag antibodies. Proteins were fractionated in a 4-20% SDS gel. The SS-disrupting mutations (which do not change the sequence of the encoded protein) are underlined.

(C) In vitro transcription-translation of a DNA template containing the first 94 codons of *copA*, followed by an engineered stop codon. The 16.5% Tris-Tricine SDS gel shows the [^{35}S]-labeled products corresponding to the complete 94 amino acid-long protein encoded in the 0 frame (grey arrowhead) or the 70 amino acid-long CopA(Z) produced via -1 PRF (black arrowhead). Disruption of SS in the template mSS by two synonymous mutations (shown in panel B) prevents production of CopA(Z) in vitro.

See also Figure S2.

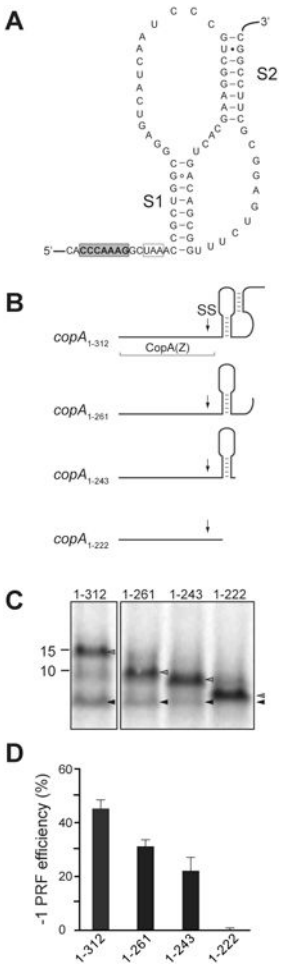

Figure 3. mRNA structure downstream of SS promotes efficient -1 PRF in the *copA* gene

(A) The predicted structure of the pseudoknot in the *copA* mRNA downstream from the SS. The slippery site is shaded in gray, the -1 frame stop codon is boxed, and stems S1 and S2 of the pseudoknot are indicated.

(B) Predicted secondary structure of the mRNA segments downstream of the SS in the 3′-truncated *copA* templates. The boundaries of the CopA(Z) coding segment is indicated and the location of SS is marked by an arrow.

(C) SDS-gel analysis of the [^{35}S]-labeled protein products expressed in vitro from the 3′-truncated *copA* templates shown in (B). Grey arrowheads indicate the bands corresponding to the full-sized 0 frame product; black arrowheads indicate CopA(Z) generated via -1 PRF.

(D) Quantification of the -1 PRF efficiency in the different 3′-truncated *copA* templates from the relative intensity of the bands indicated in (C). Error bars show standard deviation from the mean in 3 independent experiments.

See also Figure S3.

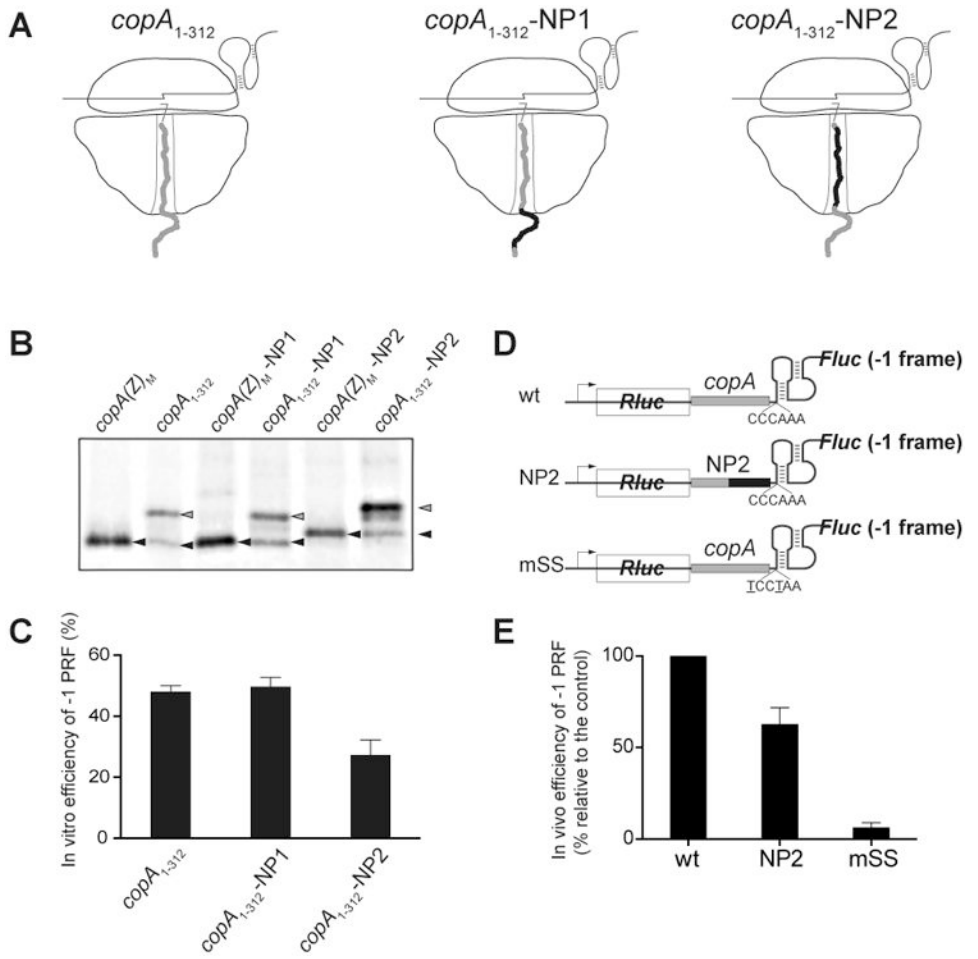

Figure 4. The CopA nascent peptide contributes to the high efficiency of -1 PRF

(A) Cartoon representation of the ribosomes translating through the *copA* SS sequence of the wt template (*copA*$_{1\text{-}312}$) or of the NP1 and NP2 mutants. The sequence of the wt CopA nascent chain is shown in grey and the mutant peptide sequence is shown in black. The nucleotide and amino acid sequences of the templates are show in detail Figure S1.

(B) Gel electrophoretic analysis of the [^{35}S]-labeled truncated CopA encoded in the 0 frame of the *copA*$_{1\text{-}312}$ wt or mutant templates (gray arrowheads) and CopA(Z) generated via -1 PRF (black arrowheads). The reference templates (M) encode the marker CopA(Z) proteins whose sequences matched those generated from the mutant templates via -1 PRF. The sequences of the reference templates are shown in Figure S1.

(C) Quantification of the -1 PRF efficiency in the different *copA* templates from the relative intensity of the bands shown in (B). Error bars show deviation from the mean in 3 independent experiments.

(D) The structures of the dual luciferase reporters containing unaltered (wt) or mutant (NP2) CopA segments. The construct carrying the *copA* sequence with the mutated SS (mSS) was used as a negative control.

(E) Efficiency of the in vivo -1 PRF in the dual luciferase reporters shown in (D). Error bars show standard deviation from the mean in 3 independent experiments.

See also Figure S1.

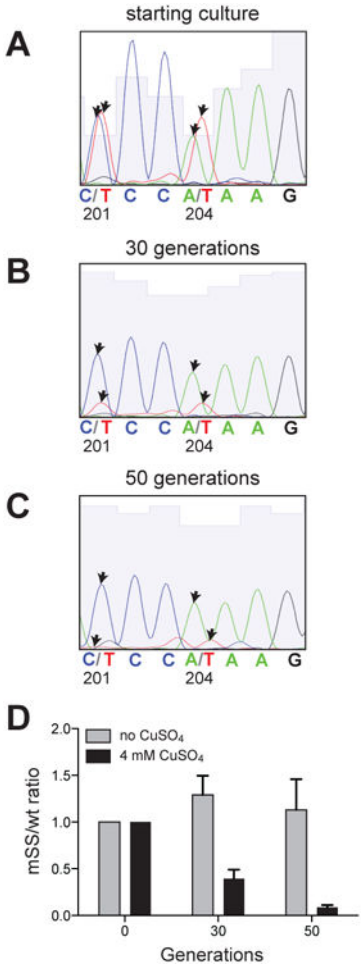

Figure 5. Production of the diffusible metal chaperone CopA(Z) helps survival during copper stress

Co-growth competition of the wt and the mSS mutant *E. coli* cells. Production of CopA(Z) in the mSS mutants was prevented by introduction of two synonymous mutations which disrupted the SS in the chromosomal *copA* gene. Equal numbers of wt and mutant cells were mixed and passaged in liquid culture in the absence or presence of toxic (4 mM) concentration of $CuSO_4$. Sequencing chromatograms of the *copA* segment PCR-amplified from the genomic DNA isolated from the co-cultures used to assess the ratio of wt and mSS cells at the (A) onset of the experiment, after (B) 30 generations or (C) 50 generations of growth in the presence of $CuSO_4$. The wt *copA* sequence contains C at position 201 and A at position 204 within the CCCAAAG slippery sequence; these residues were mutated to T in the mSS mutant. The arrows indicate the sequencing chromatograms peaks corresponding to these nucleotides.

(D) The ratios between wt and mSS cells in the co-culture were computed from the height of the chromatogram peaks. Error bars show standard deviation from the mean in 3 independent experiments.

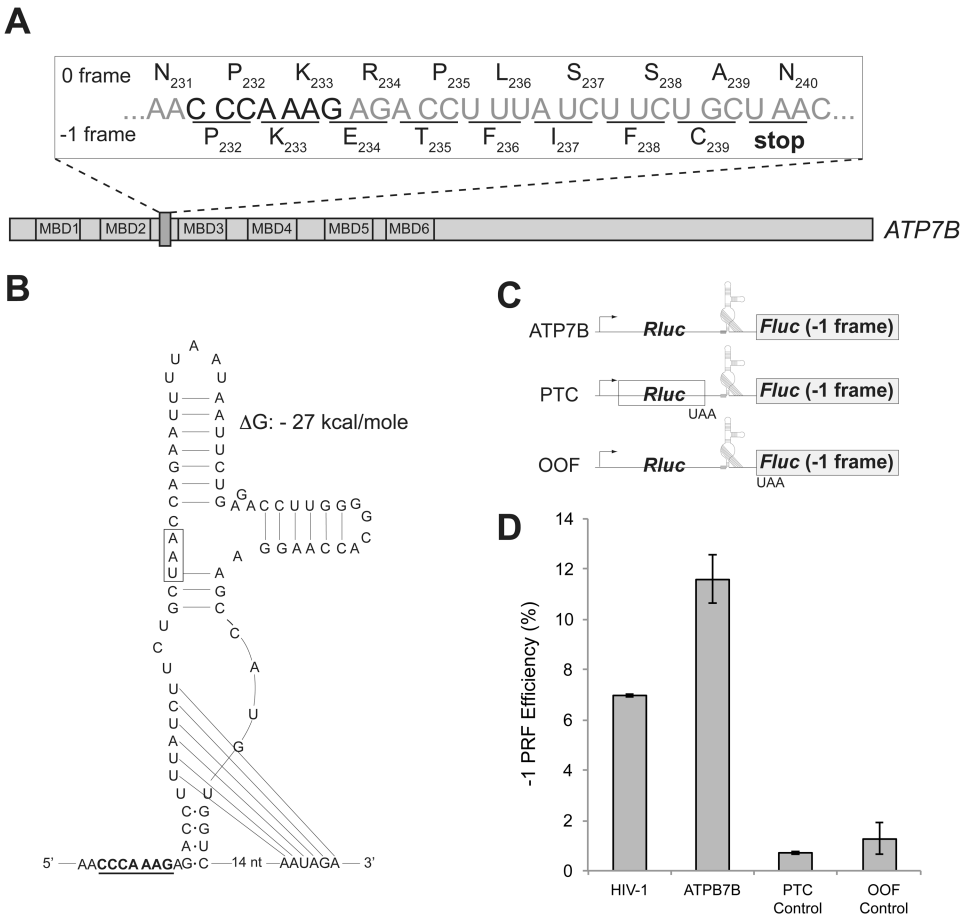

Figure 6. -1 PRF element within the human copper transporter *ATP7B* gene

(A) The location of the heptameric CCCAAAG SS of the human *ATP7B* gene. Translation in 0 frame generates the full-size ATP7B copper transporter; slippage of the ribosome into -1 frame (underlined codons) would cause termination of translation at the 240th codon (UAA) and result in production of a truncated protein consisting of the first two MBDs of ATP7B.

(B) The *ATP7B* mRNA segment downstream of the slippery sequence could fold into a PK. The SS is underlined and the -1 frame stop codon is boxed.

(C) The dual luciferase reporter constructs used to test efficiency of -1 PRF directed by the *ATP7B* SS. The minimal *ATP7B* sequence including the SS and the putative PK structure was inserted between the *Rluc* (0 frame) and the *Fluc* (-1 frame) genes. The premature termination codon (PTC) control construct carried a stop codon at the end of the *Rluc* gene. The out of frame (OOF) control construct contained a stop codon at the beginning of the -1 frame *Fluc* ORF.

(D) The -1 PRF directed by the *HIV*-1 PRF signal in comparison with the *ATP7B* PRF element within the constructs shown in panel (C) expressed in HEK293T mammalian cells. The errors bars represent standard deviation from the mean based on at least 6 independent replicates.

See also Figure S4.